ELSEVIER

FEMS Microbiology Ecology 44 (2003) 175–189

FEMS MICROBIOLOGY Ecology

www.fems-microbiology.org

Structural and functional analysis of a microbial mat ecosystem from a unique permanent hypersaline inland lake: 'La Salada de Chiprana' (NE Spain)

Henk M. Jonkers [a,*], Rebecca Ludwig [a], Rutger De Wit [b], Olivier Pringault [b,1], Gerard Muyzer [c], Helge Niemann [a], Niko Finke [a], Dirk De Beer [a]

[a] *Max Planck Institute for Marine Microbiology, 28359 Bremen, Germany*
[b] *CNRS and Université Bordeaux 1, 33120 Arcachon, France*
[c] *Kluyver Laboratory for Biotechnology, Delft University of Technology, 2628 BC Delft, The Netherlands*

Received 21 July 2002; received in revised form 4 December 2002; accepted 6 December 2002

First published online 16 January 2003

Abstract

The benthic microbial mat community of the only permanent hypersaline natural inland lake of Western Europe, 'La Salada de Chiprana', northeastern Spain, was structurally and functionally analyzed. The ionic composition of the lake water is characterized by high concentrations of magnesium and sulfate, which were respectively 0.35 and 0.5 M at the time of sampling while the total salinity was 78 g l^{-1}. Community composition was analyzed by microscopy, high-performance liquid chromatography (HPLC) pigment analyses and by studying culturable bacteria from different functional groups. Therefore, denaturing gradient gel electrophoresis (DGGE) was applied on most probable number (MPN) dilution cultures. Microscopy revealed that a thin layer of *Chloroflexus*-like bacteria overlaid various cyanobacteria-dominated layers each characterized by different morphotypes. DGGE analysis of MPN dilution cultures from distinct mat layers showed that various phylotypes of anoxygenic phototrophic, aerobic heterotrophic, colorless sulfur-, and sulfate-reducing bacteria were present. The mats were furthermore functionally studied and attention was focussed on the relationship between oxygenic primary production and the flow of carbon through the microbial community. Microsensor techniques, porewater and sediment photopigment analysis were applied in order to estimate oxygenic photosynthetic rates, daily dynamics of (in)organic carbon porewater concentration and migration behavior of phototrophs. Chiprana microbial mats produced dissolved organic carbon (DOC) both during the day and night. It was estimated that 14% of the mats gross photosynthetic production and 49% of the mats net photosynthetic production diffused out of the mat in the form of low molecular mass fatty acids, although these compounds made up only 2% of the total DOC pool. The high flux of dissolved fatty acids from the microbial mat to the water column may explain why in this system *Chloroflexus*-like bacteria proliferate on top of the cyanobacterial layers since these photoheterotrophic bacteria grow preferably on organic phototrophic exudates. Furthermore it may also explain why high numbers of viable sulfate-reducing bacteria were found in the fully oxygenated sediment surface layers. These organisms apparently do not have to compete with aerobic heterotrophic community members due to the ample availability of organic substrates. Moreover, the high production of DOC strongly indicates that the mat community was nutrient limited in its growth. Photopigment analysis revealed furthermore that chlorophyll *a* (Chl*a*) and three of its allomeres had a complementary depth distribution what suggests that the Chl*a* allomeres are functional adaptations to differences in light quality and/or quantity and may be species specific.

Keywords: Hypersaline mat; Photosynthesis; Carbon cycling; Microsensor; Denaturing gradient gel electrophoresis; Photopigment; High-performance liquid chromatography

1. Introduction

Saline and hypersaline inland lakes occur worldwide, particularly in areas with a semiarid climate [1,2]. These lakes are extremely interesting from an ecological point of

* Corresponding author. Tel.: +49 (421) 2028 838; Fax: +49 (421) 2028 690.
E-mail address: hjonkers@mpi-bremen.de (H.M. Jonkers).

[1] Present address: Centre IRD de Nouméa, 98848 Nouméa Cedex, New Caledonia.

0168-6496/03/$22.00
doi:10.1016/S0168-6496(02)00464-6

view because many harbor biological communities which are often characterized by the presence of unique species. Biodiversity in such lakes varies due to differences in environmental conditions and specific lake characteristics such as local climate, lake size, depth, and lake water salt composition. The occurrence of natural hypersaline inland lakes in Western Europe is confined to the semiarid endorheic regions of the Iberian Peninsula [3]. Here, most lakes are shallow and non-permanent with a wide spectrum of ionic types, ranging from sodium chloride- and sodium sulfate-dominated (Andalucian lakes) to sodium chloride- and magnesium sulfate-dominated ones (Aragón and La Mancha lakes).

The lake, 'La Salada de Chiprana' located in the central Ebro Basin in northern Spain, stands out in being the only permanent hypersaline lake in Western Europe. This unique lake with a maximum depth of 5.6 m and an average salinity of 78‰ dominated by magnesium sulfate, is part of a complex of lakes in the Chiprana-Caspe region. A paleolimnological analysis has shown that the current hydrology of the lake is the result of the subtle interaction between human and natural factors. During the last millennium the lake changed from a typical playa lake with temporary water, into a permanent deep lake particularly because of deforestation, introduction of agriculture and irrigation since the 17th century [4]. Extensive *Microcoleus chthonoplastes* microbial mats and macrophyte prairies were observed in the late 1980's [5]. However, the ecosystem suffered from heavy eutrophication in the early 1990's when the lake received particularly high quantities of nutrient-rich fresh water from the adjacent shallow lake 'Laguna de las Roces' through a small canal [4,6]. In concert with a drastic decrease of the water column grazer *Artemia parthenogenetica* this had a very negative impact on water column transparency and therefore on the distribution of macrophytes and on the structural integrity of the microbial mats [6]. These observations led the local authorities to develop a management plan, which included a restriction of the nutrient-rich fresh water inputs into the lake. After the particularly dry year 1995, water column transparency quickly recovered [4] and we observed extensive and healthy *M. chthonoplastes* mats since the summer of 1996. Nowadays, several distinct lacustrine sub-environments are recognized each characterized by specific biological assemblages: (1) littoral areas characterized by reed *Phragmites* spp. beds; (2) a sub-littoral area down to a depth of 1.5 m dominated by benthic microbial mat communities interspersed with charophyte *Lamprothamnium papulosum* and macrophyte *Ruppia maritima* L. var. *maritima* meadows; (3) an anoxic hypolimnion characterized by blooms of the green sulfur bacterium *Chlorobium vibrioforme* [4–7]. 'La Salada de Chiprana' with its unique but fragile ecosystem was included in the Ramsar Convention in 1994 because of its particular ecological value [6] and the regional government (Diputación General de Aragón, Zaragoza) recently developed a management plan in cooperation with local farmers to conserve and protect the lake.

In this study the benthic microbial mat community that dominates the sub-littoral area of Lake Chiprana was structurally and functionally analyzed. Main goal of this study was to make an ecological analysis of this ecosystem, i.e. relating the community structure to its functioning. The in situ primary production of the oxygenic phototrophic community was related to the dynamics and flow of dissolved organic carbon. The community structure was analyzed using a combination of microscopic, culturing and molecular techniques, while community functioning was studied by application of in situ microsensor techniques in combination with (in)organic carbon analyses of porewater and HPLC analysis of photopigments of the microbial mat ecosystem.

2. Materials and methods

2.1. Study area and sampling periods

'La Salada de Chiprana' (41°14′30″N, 0°10′50″W) has a total surface of 31 ha. The lake lies on the Upper Oligocene–Miocene Caspe Formation that is mainly composed of sand and silt stones. The lake's hydrology is governed by high evapotranspiration (1000–1500 mm year^{-1}), low rainfall (300–350 mm year^{-1}), water runoff, irrigation returns and groundwater flow. The latter is thought to be the main source of the lake's solutes due to the dissolution of the carbonate and evaporite rocks of the area's Tertiary formations, resulting in an ionic composition dominated by magnesium sulfate [4,5]. The average salinity of the lake water is around 78‰ but was reported to decrease significantly during occasional periods of heavy rainfall [5,6]. For this study, the lake was visited in successive autumn and spring seasons, October 2000 and May 2001 respectively, during which microsensor in situ measurements were performed. Samples taken for further laboratory analysis were directly frozen on site and transported to the laboratory in liquid nitrogen cooled transportation vessels (CP100, Taylor-Wharton, USA).

2.2. Structural community analyses

2.2.1. Macroscopic and microscopic observations

Vertical cuts of freshly collected mats (October 2000 and May 2001) were macroscopically photographed with a digital camera in order to visualize the distinct colored layers of which the mats consisted. Subsequently, with the aid of binoculars and watchmaker forceps, microscopic slides were prepared from subsamples taken from these distinct depth layers. The volumetric abundances of morphologically clearly distinguishable phototrophic community members in these preparations (cyanobacteria, diatoms and filamentous *Chloroflexus*-like bacteria) were

subsequently estimated by bright field, phase contrast and fluorescence microscopy. For the latter, microscopic preparations were excited with blue (450–495 nm) or green (546 nm) light and emitted light was cutoff with filters for wavelengths below 520 and 590 nm respectively, facilitating the distinction between chloroplast-containing algae and phycobiliprotein-containing cyanobacteria respectively.

2.2.2. Numerical estimation of culturable bacteria

The abundances of culturable bacteria belonging to four different functional groups, aerobic heterotrophic bacteria, sulfate-reducing bacteria, anoxygenic phototrophic sulfur bacteria and colorless sulfur bacteria, were estimated in freshly collected mats (October 2000) by the most probable number (MPN) methodology. Duplicate microbial mat cores were randomly collected using 25 mm diameter perspex sediment corers. The top 6 mm of these cores were sliced in two 3 mm thick layers representing the photic (top layer) and equally thick aphotic zone of the microbial community. Slices were fragmented by cutting, suspended in nine volumes of 0.2 μm filtered and autoclaved Chiprana lake water. Suspensions were further homogenized by three cycles of rigorously vortexing (2 min) followed by sonication (10 s) in a 50 W ultrasonic bath. Microtiter plates (8×12 wells, Merck, Germany) were filled with MPN medium amended with functional group-specific substrates (see below for medium composition). The first row of wells (representing eight replicates) was inoculated with 10% (volume) microbial mat suspension (10^{-2} dilution) followed by serial dilution up to the 10^{-12} dilution level, leaving the last row as blanks (abiotic controls). Plates were incubated either aerobically (aerobic heterotrophs and colorless sulfur bacteria) or anaerobically using the Merck anaerocult system (sulfate-reducing and anoxygenic phototrophic sulfur bacteria). All plates were incubated at room temperature for 14 weeks in the dark except for the anoxygenic phototrophic bacterial plates which were incubated under a light/dark cycle of 16 h light (20 μmol photons m^{-2} s^{-1}) and 8 h darkness. Growth was followed visually by comparing medium turbidity to abiotic controls. After incubation, MPN scores representing numbers of culturable bacteria of the respective functional groups present in the original microbial mat, were calculated using the MPN computer program of Clarke and Owens [8].

MPN medium was composed of 50% 0.2 μm filtered and autoclaved Chiprana lake water and 50% artificial medium. The latter contained per liter of Milli-Q water: NaCl (17.5 g), $MgSO_4 \cdot 7H_2O$ (78.0 g), NH_4Cl (0.2 g), KH_2PO_4 (0.02 g), $CaCl_2 \cdot 2H_2O$ (0.225 g), KCl (0.2 g), Na_2CO_3 (2.0 g) and ethylenediamine tetraacetic acid (EDTA) trace element solution of Widdel and Bak [9] (1 ml l^{-1}). This medium was amended with growth factors and substrates for the respective functional groups. For sulfate-reducing bacteria: Wo/Se solution and vitamin solution of Heijthuijsen and Hansen [10] (1 ml l^{-1}), lactic acid (15 mM) and acetic acid (15 mM). For anoxygenic phototrophic bacteria: cyanocobalamine (vitamin B12, 20 μg l^{-1}), hydrogen sulfide (1.6 mM) and acetic acid (0.8 mM). For colorless sulfur bacteria: cyanocobalamine (20 μg l^{-1}) and thiosulfate (6.4 mM). For aerobic heterotrophic bacteria: cyanocobalamine (20 μg l^{-1}) and either glycolic acid (20 mM) or a mixture of glycolic acid, glucose, lactic acid and acetic acid (5 mM each). The pH of all media was adjusted to 8.2.

2.2.3. Molecular characterization of MPN dilutions

The within functional group diversity of bacteria was studied in MPN culture samples by application of the polymerase chain reaction (PCR) followed by separation of DNA products using denaturing gradient gel electrophoresis (DGGE). Culture samples from moderate (10^{-4}) and highest positive (10^{-6}, 10^{-7} or 10^{-8}) MPN dilution levels were analyzed. Therefore 0.2 ml culture samples were taken, centrifuged (10 min at 16 000×*g*) followed by resuspension of the pellet in 30 μl TE buffer (10 mM Tris–HCl, 1 mM EDTA; pH 8). DNA was extracted by subjecting cell suspensions to five cycles of freeze-thawing followed by heating for 10 min at 95°C. Mixtures of 16S rRNA genes in these samples were PCR amplified with GM5 forward (with GC clamp) and 907 reverse primers resulting in 0.5 kb fragment lengths and DGGE was subsequently performed as described by Muyzer et al. [11].

2.3. Functional community analysis

2.3.1. In situ microsensor measurements

In situ microbial mat profiles of oxygen concentration (October 2000) and in situ profiles of oxygen, pH, oxygenic gross photosynthesis and sulfide concentrations (May 2001) were measured during 24 h cycles. Clark-type amperometric oxygen microsensors (10 μm tip diameter), and potentiometric pH and sulfide (S^{2-}) minisensors (100 μm tip diameter) were applied (see [12,13] for detailed description of used sensors). The latter two sensors were glued in steel needles because unprotected glass pH microsensors broke always on calcium carbonate precipitates in the microbial mats, whereas use of amperometric H_2S sensors was hampered by high ultraviolet (UV) light intensities during in situ measurements. In situ profiles were obtained by fixing microsensors in a manual micromanipulator connected to a heavy stand. The setup was positioned on the sediment surface of a 20 cm deep submerged microbial mat. Gross photosynthesis profiles were obtained by application of the light/dark shift method. For these measurements oxygen microsensors with a response time of less than 0.2 s were used [14]. Darkening was done by rapidly covering the setup and underlying mat with a black cloth cover for 5-s time intervals. The initial decrease in oxygen concentration was registered on a strip chart recorder.

2.3.2. Photopigment quantification

Photopigments were analyzed by HPLC. 1 mm thick slices of microbial mats sampled in October 2000 were analyzed in Arcachon following the procedure described by Buffan-Dubau et al. [15]. In summary, the pigments were extracted with cold acetone and four successive extractions were pooled. Pigment extracts were methylated with diazomethane, subsequently dried by centrifugation under vacuum and dissolved in solvent A. A binary gradient (solvent A = 50% methanol, 45% acetonitrile+5% aqueous solution of 0.05 M ammonium acetate; solvent B: 80% ethyl acetate, 19% methanol and 1% acetonitrile) was applied, pigments were separated on a Lichrospher 100RP (250×4 mm, 5 μm) column, and a ThermoSeparation Products (Les Ulis, France) TSP UV6000 diode array spectrophotometer was used as a detector. The TSP UV6000 was programmed to obtain the on-line absorption spectra from 320 to 800 nm, and chromatograms were plotted at 440 nm (detection of carotenoids and chlorophylls) and at 664 nm (specific detection of chlorophylls and degradation products [15]). Pigments were identified by comparison with authentic standards if available. An extract of a culture of *Chlorobium tepidum* ATCC was used as source for bacteriochlorophyll *c* homologs.

A higher depth resolution of the photopigments was achieved on samples from May 2001 using HPLC equipment in Bremen. The vertical distribution of photopigments in the microbial mats was determined in sediment cores taken at 5 a.m. and 5 p.m. in order to study diel migration phenomena. These cores were immediately frozen on site in liquid nitrogen and transported to the laboratory. The top 6 mm of the frozen cores were sliced in 200 μm thick layers with the aid of a Cryomicrotom (Microm HM 505E) at −30°C. Individual slices were weighed and immediately extracted in 1.2 ml 100% methanol. For the quantification of zeaxanthine slices were washed in 2 ml saline water (80 g NaCl per l Milli-Q water) prior to extraction. This washing step was necessary because during direct extraction zeaxanthine was degraded by an unknown compound present in the sediment porewater in deeper sediment layers. Photopigments in methanol extracts were subsequently separated on a Waters HPLC (2690 Separation Module) equipped with a Eurospher-100 C18, 5 μm Vertex column (Knauer, Berlin, Germany) according to the method of Wright et al. [16]. Absorption spectra of separated compounds were measured on a Waters 996 Photo Diode Array (PDA) detector and pigment quantity and purity were checked by comparing peak areas, peak retention times, and absorption spectra to pigment standards. The following pigment standards were used (in brackets retention time in min on our HPLC system): peridinin (11.5), fucoxanthin (12.4), chlorophyll *b* (Chl*b*) (16.8), zeaxanthine (17.0), lutein (17.2), chlorophyll *a* (Chl*a*) (17.7) and β-carotene (20.4). Standards were purchased from Sigma, USA or DHI Water and Environment, Denmark. Three allomeres of Chl*a* were detected in field samples. These allomeres had identical absorption spectra but different retention times as Chl*a*. Retention times were 15.1, 17.4 and 18.1 min and these allomeres are annotated in the following as Chla_1, Chla_2 and Chla_3 respectively. Allomeres were quantified using Chl*a* as standard.

2.4. Chemical analysis of porewater

The daily dynamic of dissolved organic carbon (DOC) and dissolved inorganic carbon (DIC) concentrations in the microbial mat porewater was analyzed in order to relate this to the mat photosynthetic activity. In May 2001 water column samples and triplicate mat cores were taken at 5 a.m. and 5 p.m. The sediment cores were immediately sliced on site in distinct layers (0–2 mm, 2–4 mm and 4–8 mm) followed by centrifugation of the sediment slices (10 min at 6000×*g*). Supernatant (porewater) aliquots were immediately frozen in liquid nitrogen. The concentration of dissolved organic and inorganic carbon of these samples was measured with a Shimadzu TOC-5050A Total Organic Carbon Analyzer in connection with a Shimadzu ASI-5000A Autosampler. The samples were five-fold diluted with Milli-Q water prior to analysis.

Porewater and water column samples were additionally analyzed for low molecular mass fatty acids (formic, glycolic, acetic, lactic, propionic, butyric, iso-butyric, valeric and iso-valeric acid). Fatty acids were prior to analysis derivatized with phenylhydrazine and quantified by HPLC according to the method described by Albert and Martens [17].

The ionic composition of Chiprana lake water (October 2000 and May 2001) was determined in 0.2 μm filtered water samples by ion chromatography on a Dionex DX 500 Chromatograph according to the method of Schippers and Jørgensen [18]. Calcium concentrations were checked and confirmed by atomic absorption spectrometry (AAS).

3. Results

3.1. Ionic composition of Chiprana lake water

The salt composition of Chiprana lake water did not vary much during the autumn and spring season of the years 2000 and 2001, but differed markedly from 'average' seawater, not only in terms of total salinity but also in ratio of the respective ions (Table 1). Chiprana water appeared to be particularly rich in calcium, magnesium and sulfate, with respective concentrations being 2, 7 and 17 times higher as seawater.

3.2. Structural analysis of the microbial mat community

3.2.1. Macroscopic and microscopic analyses

The macroscopically clearly visible vertical layering of

Table 1
Salt composition of Chiprana lake water and seawater

Seawater[a]:		Chiprana water: October 2000	Chiprana water: May 2001
Ions:	mM	mM	mM
K^+	10	5	6
Mg^{2+}	53	322	375
Na^+	468	497	515
Ca^{2+}	10	18	20
Cl^-	545	309	356
SO_4^{2-}	28	500	446
Cations	604	1182	1311
Anions	601	1309	1248
Ions:	g l^{-1}	g l^{-1}	g l^{-1}
K^+	0.4	0.2	0.2
Mg^{2+}	1.3	7.8	9.1
Na^+	10.8	11.4	11.8
Ca^{2+}	0.4	0.7	0.8
Cl^-	19.5	11	12.7
SO_4^{2-}	2.7	48.1	42.9
Total	35.1	79.2	77.5

Chiprana water appeared to be particularly rich in magnesium, calcium and sulfate.
[a]Seawater values taken from Stumm and Morgan [35].

the Chiprana lake microbial mat is shown in Fig. 1. Microscopic observations revealed a high diversity of morphologically distinct autofluorescent organisms. These are in the following described according to morphology, i.e. unicellular or filamentous, and cell size (individual cells, width × length). Biomass of morphotypes in the microscopic preparations was estimated in terms of volumetric percentage. The orange-brown 0.5 mm thick top layer (layer 1, see Fig. 1) was mainly composed of *Chloroflexus*-like thin (0.5–1 × > 100 μm) filamentous bacteria. These were only weakly autofluorescent in the near infrared light range and their biomass was estimated to make up 90% of the total biomass in this layer. Other conspicuous autofluorescent organisms in this layer were two types of diatoms (*Nitzschia* sp.: 4 × 70 μm, 5–10%; and *Navicula* sp.: 20 × 80 μm, 1% respectively), and three types of cyanobacteria, one Halothece-like unicellular (1 × 1–2 μm; 1%), and one *Microcoleus*-like (2 × 5 μm, 1%, annotated as filamentous cyanobacterium type 2) and one *Pseudoanabaena*-like (1.5–2 × 4–5 μm; 2–5%, annotated as type 5) filamentous bacterium. The underlying layer (layer 2) had a thickness of about 1 mm and was brightly green. This layer consisted predominantly of four types of filamentous cyanobacteria: three *Microcoleus*-like (1 × 4 μm, 80%, annotated as type 3; 2 × 5 μm, 2–5%, type 2 and 5 × 10 μm, 5–10%, annotated as type 1 respectively) and one *Pseudoanabaena*-like (1.5–2 × 4–5 μm, 2–5%, type 5) bacterium. Layers 2 and 4 were separated by a clearly visible calcium carbonate layer (layer 3). Layer 4 was a 4 mm thick brown gelatinous layer, interspersed with calcium carbonate crystals, and was dominated, like layer 2, by a *Microcoleus*-like filamentous cyanobacterium (80%,

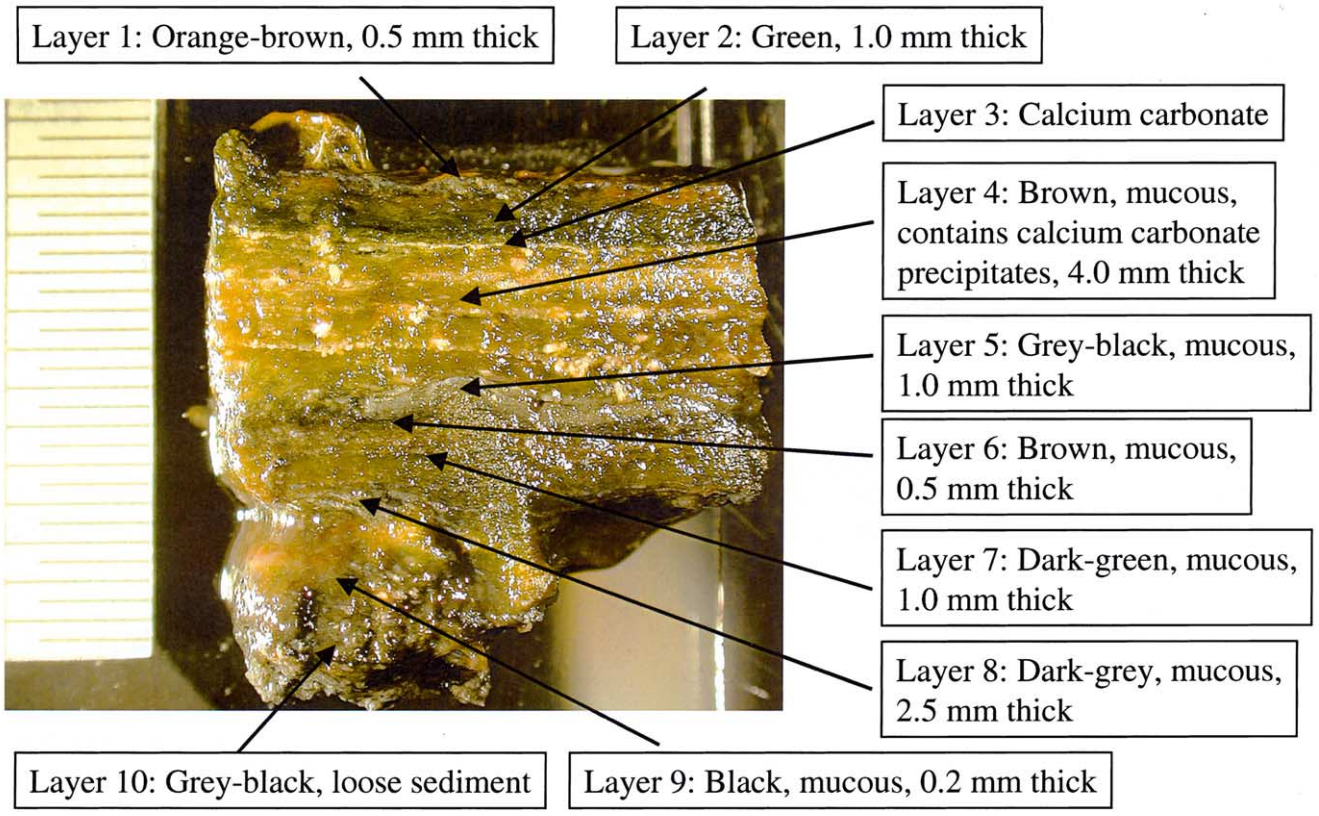

Fig. 1. Photograph of a vertical cut of a Chiprana lake microbial mat. Distinct layers are clearly visible. See Section 3 for a microscopic description of cyanobacterial and algal morphotypes present in the respective layers.

type 3) with type 1 (2%), and a Halothece-like unicellular (1×1 μm; 1%) and two types of *Gloeocapsa*-like (2×2 μm, 2% and 5×7 μm, 2%) cyanobacteria also being present. The underlying 1 mm thick layer 5 was grayish-black and had a cyanobacterial composition similar to layer 4. Below layer 5 the mat layering seemed to repeat itself with layers 6, 7, 8 and 9 corresponding to layers 1, 2, 4 and 5. However, the autofluorescence of the cyanobacteria in the layers 6–9 was much weaker and present diatom frustules were predominantly empty. In layer 6 a low abundant (<1%) morphologically different type of filamentous bacterium with clearly separated individual cells was detected (1×2 μm, annotated as type 4). In the whole mat, 11 different morphotypes of autofluorescent organisms could microscopically be detected, two diatoms, one *Chloroflexus*-like filamentous bacterium, two *Gloeocapsa*-like cyanobacteria, one Halothece-like unicellular cyanobacterium and five filamentous cyanobacteria.

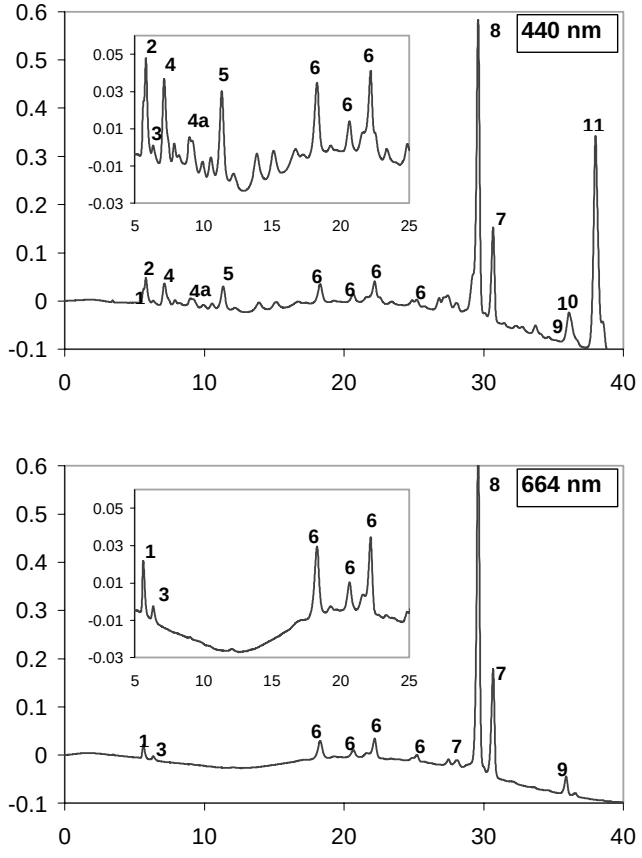

Fig. 2. HPLC chromatograms of a pigment extract of the top mm of the mat sampled in October 2000. *Chloroflexus*-like filamentous bacteria dominate the mat surface layer what is reflected by the presence of BChl*c*.

3.2.2. Pigment analyses of the mat top mm

Pigment chromatograms of the top mm of the mat are shown in Fig. 2. Fucoxanthin and chlorophyll *c* reflect the presence of diatoms, while myxoxanthophyll and zeaxanthine reflect the presence of the cyanobacteria. The latter compound is also present in some green algae, but because the green algal pigments chlorophyll *b* and lutein were below the limit of detection, we can safely assume that the bulk of zeaxanthine originated from cyanobacteria. Other major carotenoids comprised γ-carotene and β-carotene. Chlorophyll *a* (Chl*a*) was the major peak. Two chlorophyll *a*-like pigments were detected that likely correspond to a chlorophyll *a*-allomer and a chlorophyll *a* epimer [19]. Chlorophyllide *a* and phaeophytin *a*, but no phaeophorbides, were detected as degradation products arising from Chl*a*.

A group of peaks eluting between 18 and 26 min were identified as bacteriochlorophyll *c* (BChl*c*). The absorption spectrum and the retention time of these compounds corresponded to the secondary BChl*c* homologs of *C. tepidum*. The retention times were longer than for the farnesol-esterified BChl*c* homologs (BChlc_F), which are the main homologs in *C. tepidum*. This indicates that the BChl*c* homologs were more hydrophobic than the BChlc_F homologs and therefore esterified with another alcohol [20,21]. HPLC-mass spectroscopy (MS) analysis is requested for identification of the esterifying alcohol [21,22]. The BChl*c* homologs most likely originated from *Chloroflexus*-like filamentous bacteria, they were most abundant in the top layer and decreased strongly with depth (data not shown).

3.2.3. Estimation of diversity and number of culturable bacteria

In addition to the autofluorescent microbial mat inhabitants, the diversity and number of culturable microorganisms of four different functional groups (aerobic heterotrophic bacteria, sulfate-reducing bacteria, anoxygenic phototrophic bacteria and colorless sulfur bacteria) were estimated by a combination of the MPN methodology and PCR-DGGE. The functional group of anoxygenic phototrophic bacteria was dominated by purple sulfur bacteria. Fig. 3 depicts the numerical (MPN) estimates of bacteria of the four functional groups in the photic (0–3 mm) and aphotic (3–6 mm) layers of the mat. Numbers of culturable bacteria of these four functional groups appeared to be hardly different between the two layers. Aerobic heterotrophic bacteria were numerically dominant in both layers followed by smaller population sizes of colorless and purple sulfur bacteria with the sulfate-reducing bacteria being numerically the smallest population. The latter group, however, was still present in significant numbers both in the photic and the aphotic zone. Not shown in Fig. 3 are the numbers of the aerobic heterotrophs cultured on glycolic acid only, because this group represents a subpopulation of the aerobic heterotrophs cultured on a

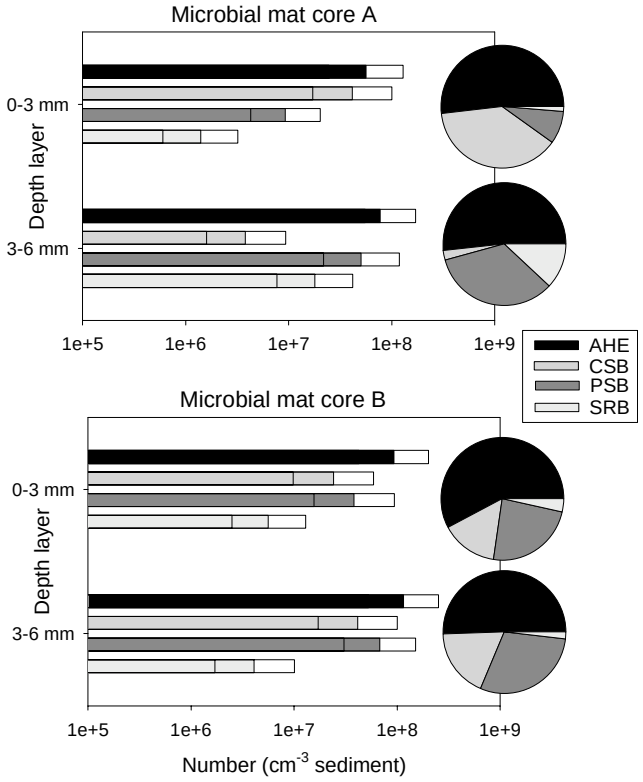

Fig. 3. Most probable number estimates in duplicate cores of aerobic heterotrophic, sulfate-reducing, anoxygenic phototrophic and colorless sulfur bacteria in the photic (0–3 mm) and aphotic (3–6 mm) layers of the Chiprana lake microbial mat. Pie charts show relative abundance of estimated groups.

mixture of organic substrates (glycolic acid, glucose, acetic acid and lactic acid). The MPN estimate of the former group was 25% lower than of the latter group. This means that 75% of the aerobic heterotrophic bacteria that grew on the substrate mixture can grow on glycolic acid as sole carbon source.

An estimate of the within functional group diversity was made by application of PCR-DGGE on the MPN series. Fig. 4 shows the obtained DGGE patterns of the intermediate (10^{-4}) and highest positive (10^{-5}–10^{-8}) MPN dilution levels. Assuming that the individual distinguishable bands (phylotypes) represent distinct species, it can be concluded that the within group diversity is considerable. However, these results should be interpreted with some care because the possible occurrence of multiple copies of 16S rRNA genes in individual species may result in an increased number of phylotypes and therefore in an overestimation of the microbial biodiversity. Generally, different phylotypes were found in the photic and aphotic mat layers indicating that different species dominated the respective layers. Furthermore, phylotypes from the highest positive dilution levels were generally different from those that appeared in the lower (10^{-4}) dilution level. An interesting phenomenon occurred in the aerobic heterotrophic cultures. Here, growth on glycolic acid as sole substrate resulted in the appearance of a higher number of phylotypes than with growth on a mixture of substrates. The apparent diversity of (micro)organisms of different functional groups of Chiprana lake microbial mats is summarized in Table 2.

Table 2
Apparent diversity of functional groups of (micro)organisms in Lake Chiprana microbial mats

Functional group:				Number of morphotypes (m) or phylotypes (p)[a]:
Oxygenic phototrophs				
Diatoms:				2 (m)
Nitzschia sp.	(4×70 μm)	5%	layer 1	
Navicula sp.	(20×80 μm)	1%	layer 1	
Cyanobacteria:				8 (m)
Halothece-like unicellular	(1×1–2 μm)	1%	layer 1, 4	
Gloeocapsa-like	(2×2 μm)	2%	layer 4	
Gloeocapsa-like	(5×7 μm)	2%	layer 4	
Microcoleus-like type 1	(5×10 μm)	5–10%	layer 2	
Microcoleus-like type 2	(2×5 μm)	2–5%	layer 2	
Microcoleus-like type 3	(1×4 μm)	80%	layer 2, 4	
Microcoleus-like type 4	(1×2 μm)	1%	layer 6	
Pseudoanabaena-like type 5	(1.5×4 μm)	2–5%	layer 2	
Anoxygenic phototrophic bacteria				
Chloroflexus-like bacteria	(1× >100 μm)	90%	layer 1	1 (m)
Purple sulfur bacteria				6 (p)
Aerobic heterotrophic bacteria				5 (p)
Colorless sulfur bacteria				7 (p)
Sulfate-reducing bacteria				9 (p)

Number of phylotypes correspond to the number of distinguishable DGGE bands (see also Fig. 4). Individual cell sizes of the different morphotypes and estimated biomass in the microbial mat layer (see Fig. 1) where they appeared most prominently are given.
[a]Morphotypes determined by microscopy and phylotypes by PCR-DGGE (see Section 2).

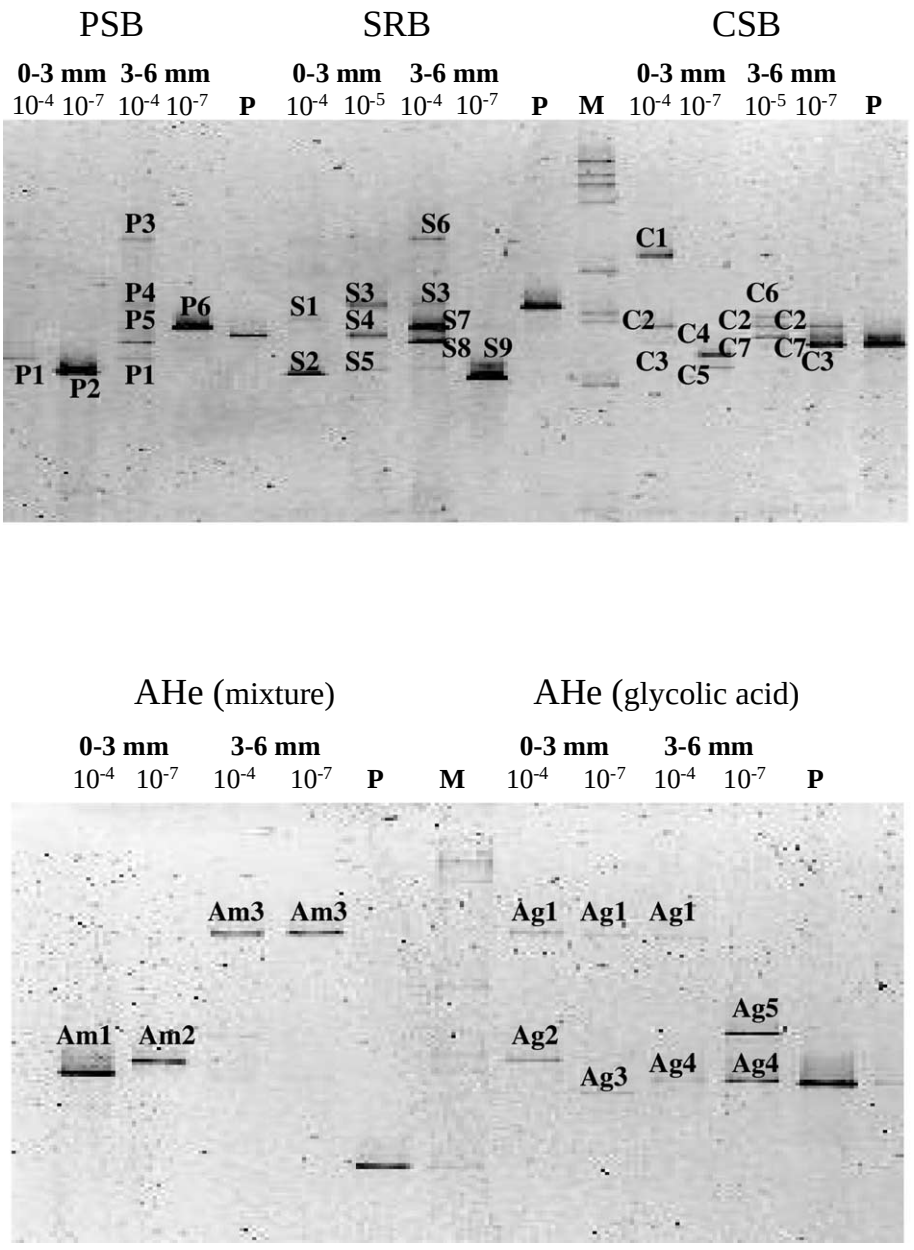

Fig. 4. Negative images of DGGE separation patterns of PCR-amplified 16S rRNA gene fragments from MPN enrichment cultures. Functional group, depth layer (0–3 or 3–6 mm) and MPN dilution levels are shown above the lanes. *Pc* and *M* refer to positive controls and mass standards respectively. Distinct band (phylotypes) numbers refer to the specific functional group (P, purple sulfur bacteria; S, sulfate-reducing bacteria; C, colorless sulfur bacteria; Am, aerobic heterotrophs enriched on mixed organic substrates; Ag, aerobic heterotrophs enriched on glycolic acid) and to the distinct migration position in the gel.

3.3. Functional analysis

3.3.1. Photosynthesis rates and daily dynamics of oxygen, sulfide and pH

The in situ measurements of oxygen dynamics during a daily cycle are presented in Fig. 5. The oxygen concentration rapidly built up directly after sunrise and reached over five times air saturation (1 mM oxygen) already at 10 a.m. at a light intensity of 800 μmol photons m^{-2} s^{-1}. Subsequently, at increased light intensities, oxygen penetrated deeper in the mat and multiple concentration maxima became visible in the profiles (Fig. 5B; 1400 and 2400 μmol photons m^{-2} s^{-1}). At higher light intensities, another interesting phenomenon occurred. Oxygen not only penetrated deeper in the mat but concentrations of oxygen also decreased near the top of the mat, indicating that either downward migration of oxygenic phototrophs or photo-inhibition occurred. In the early evening the situation reversed: a decrease in light intensity resulted in higher oxygen concentrations in the mat surface layer (Fig. 5C; 2100 and 845 μmol photons m^{-2} s^{-1}), indicating upward migration or a decrease in photo-inhibition. Another

indication for vertical migration of photosynthetic activity is that oxygen concentration maxima moved from 0.5 mm depth in the morning (Fig. 5A; 09:15 h and 09:45 h) to 1.5 mm depth in the evening (Fig. 5C; 18:15 h and 18:43 h) while light intensities at these times were comparable (between 100 and 300 μmol photons m^{-2} s^{-1}).

Gross photosynthesis profiles measured in May 2001 showed double peaks at higher light intensities (870, 1240 and 1450 μmol photons m^{-2} s^{-1}), with peak maxima around 1 and 2.5 mm depth, corresponding to the double peaks in the oxygen profiles (Fig. 6). Calculated areal gross photosynthetic rates (sum of depth-integrated gross volumetric values) amounted to 0.05, 0.21, 0.44 and 0.29 nmol O_2 cm^{-2} s^{-1} at light intensities of 125, 870, 1240 and 1450 μmol photons m^{-2} s^{-1} respectively. The latter value indicates that at high light intensities photo-inhibition occurred. A comparison between oxygen dynamics in May and October revealed little seasonal variation. While the oxygen penetration depths were similar (3–4 mm depth), the oxygen concentration maximum was highest in October, i.e. 1400 μM and 900 μM in October and May, respectively. Sulfide (S^{2-}), measured with a needle minisensor, could be detected near the sediment surface during the night (at 1 mm depth) but only in deeper mat layers during the day (>4 mm depth; results not shown). Maximal total sulfide concentrations (H_2S, HS^- and S^{2-}) in the dark, calculated using the S^{2-} and depth corresponding pH values according to Revsbech et al. [23], amounted to 2 mM. The pH of Chiprana lake water was 8.5 but increased in the photosynthetically active layer of the mat during the day to values above 9. The pH decreased in deeper mat layers during the day as well as in the whole mat during the night to values around 7.5. The water temperature was measured directly above the microbial mat sediment surface. The temperature increased from lowest night time values (15 and 25°C in October and May, respectively) to highest midday time values (19 and 28°C in October and May, respectively). The higher water temperatures in May resulted in lower peak values of oxygen concentration in the photic zone possibly by a combination of lower solubility of oxygen in warmer water and increased respiration.

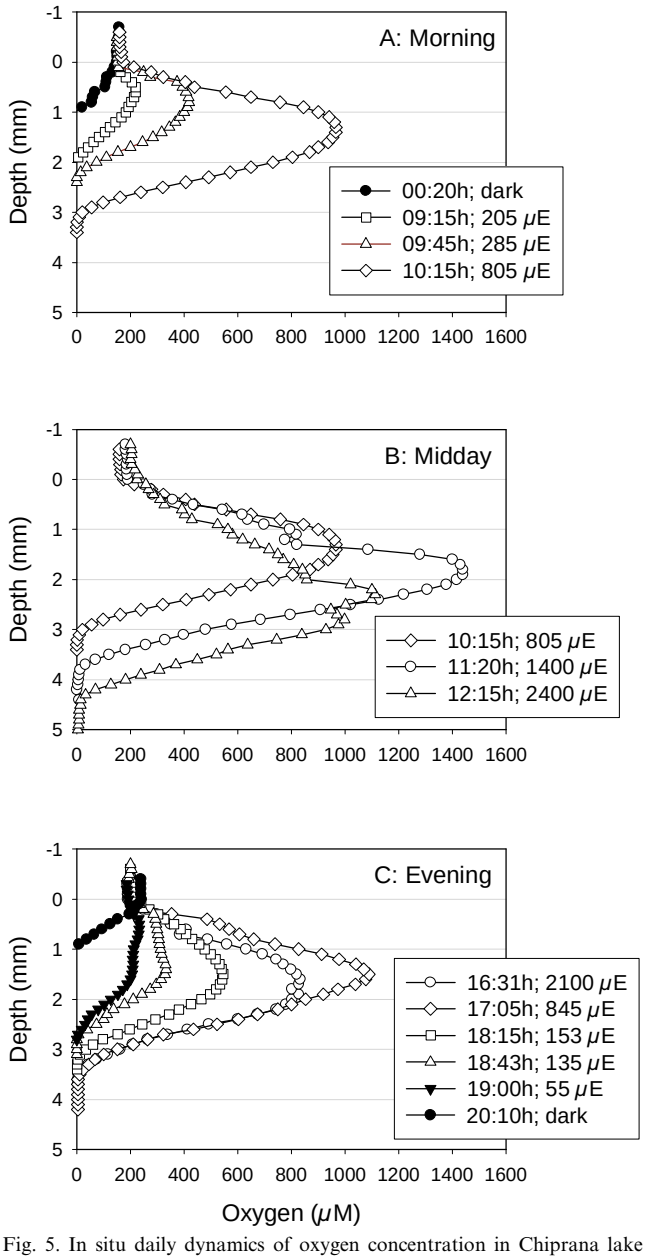

Fig. 5. In situ daily dynamics of oxygen concentration in Chiprana lake microbial mat (October 2000). Midday profiles (B) show that at higher light intensities (1400 and 2400 μmol photons m^{-2} s^{-1}) multiple oxygen concentration maxima occur but that the oxygen concentration in the surface layer (0–2 mm) simultaneously decreases.

3.3.2. Depth distribution of photopigments

In order to determine diurnal vertical migration behavior of phototrophic organisms, the photopigment distributions in microbial mat cores taken at 5 a.m. and 5 p.m. were compared. Photopigment profiles of Chl*a* and three of its allomeres, fucoxanthin, zeaxanthine and β-carotene, diagnostic pigments for oxygenic phototrophs, diatoms, cyanobacteria and general phototrophs respectively, are shown in Figs. 7 and 8. Lutein, Chl*b* and peridinin, signature pigments for green algae (lutein and Chl*b*) and dinoflagellates (peridinin), were below detection limit (0.1 μg g^{-1} sediment). The vertical distribution of Chl*a* and its allomeres (Fig. 7) show that the individual compounds have distinct distributions and, moreover, that their depth maxima during the day are complementary with respective maxima at 1, 3 and 6 mm (Chl*a*), 4 mm (Chla_1), 2–3 and 6 mm (Chla_2), and 1.5 and 5.5 mm (Chla_3). Comparison of day and night profiles shows that maxima or part of the maxima of the day profiles are shifted upwards with 1–2 mm in the night profiles. The profiles of the carotenoids fucoxanthin, zeaxanthine and β-carotene, however, do not show clear differences between day and night depth distributions (Fig. 8).

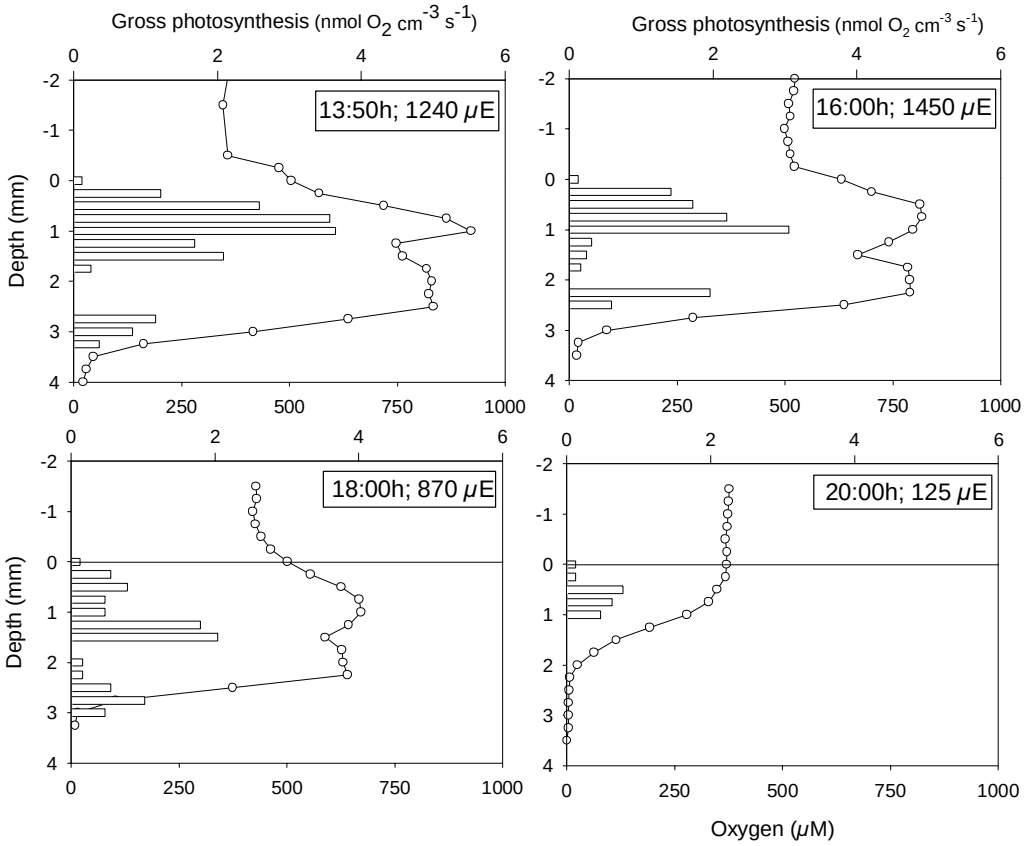

Fig. 6. In situ oxygen and photosynthesis depth profiles (May 2001). Oxygen concentration maxima at higher light intensities coincide with photosynthesis maxima.

3.4. Daily dynamics in porewater DIC, DOC and fatty acids: flux calculations

Dynamics in microbial mat porewater concentrations of dissolved organic (DOC) and inorganic carbon (DIC) were studied because these may reflect autotrophic and heterotrophic activities. The 0–2 mm depth layer showed the highest concentration differences between day and night (Fig. 9). The lowest DIC and highest DOC concentrations were measured in this layer during the day, indicating a respective flux of DIC into and flux of DOC out of this layer. The DOC concentration difference between the 0–2 mm depth layer and the water column was much higher than between the 0–2 and 2–4 mm depth layer. This indicates that the main flow of DOC was primarily towards the water column. The chemical composition of the DOC pool remains largely unknown since in this study only short-chain fatty acids were measured. Significant concentrations of formic, acetic, lactic and propionic acid could be detected. Concentration profiles of these compounds, except for formic acid, were similar to the DOC profiles. Low concentrations of fatty acids were found in the water column, while higher concentrations were found in the mat with maximum concentrations in the 0–2 mm depth layer. Concentrations were higher during the day, except for formic acid what was only detected in the 0–2 mm depth layer in night samples (Fig. 10). Glycolic, butyric, iso-butyric, valeric and iso-valeric acid could all be detected, but concentrations were always below 5 μM in both during day and night. The total porewater concentrations of fatty acids in terms of organic carbon in the 0–2 mm depth layer were 0.87 and 0.56 mM during day and night, respectively. These values amount to 2.2 and 1.8% of the DOC pool in this layer. An estimate of the daily fatty acid flux out of the mat can be made based on the measured concentration profiles. The flux (F) is denoted by:

$$F = D \times (\Delta C/\Delta z)$$

where D is the molecular diffusion coefficient and $\Delta C/\Delta z$ the difference in concentration between the 0–2 mm sediment layer and the overlying water. Diffusion coefficients for formic acid, acetic acid, propionic acid and lactic acid were estimated by the Wilke-Chang technique [24] and were 1.59×10^{-5}, 1.24×10^{-5}, 1.06×10^{-5} and 1.06×10^{-5} $cm^2\ s^{-1}$ respectively. The day light period was 16 h and oxygenic gross photosynthesis during this period amounted to 25.3 μmol O_2 cm^{-2} assuming an average light intensity of 1240 μmol photons $m^{-2}\ s^{-1}$. Net photosynthesis rates at 1240 μmol photons $m^{-2}\ s^{-1}$ and 0 μmol

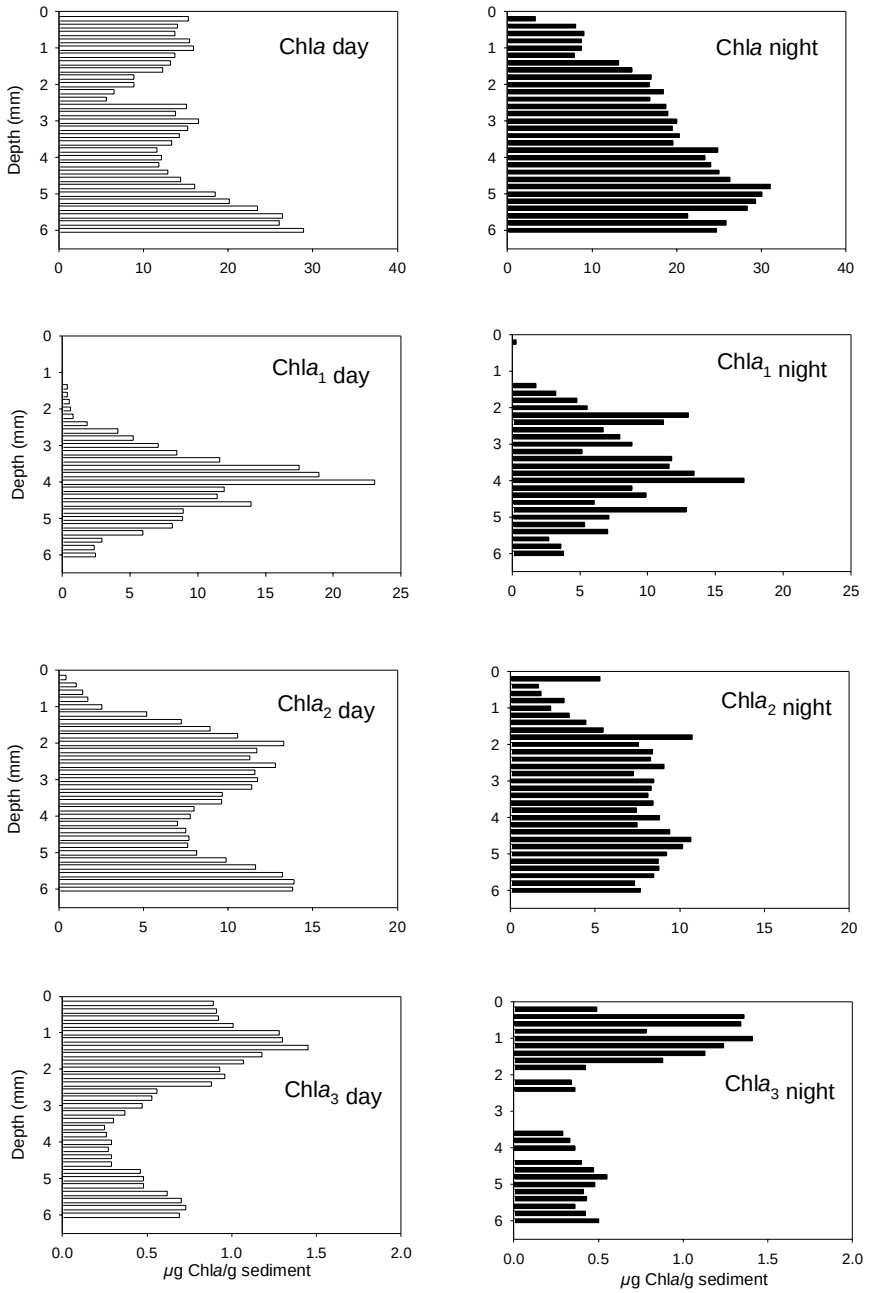

Fig. 7. Day and night depth distribution of Chl*a* and Chl*a* allomeres (Chla_1, Chla_2 and Chla_3) in Chiprana lake microbial mats showing an upward shift of photopigment distribution at night.

photons m^{-2} s^{-1} were calculated to be 0.140 and -0.025 nmol cm^{-2} s^{-1} respectively from which we calculated a daily net oxygen production rate of 7.3 μmol O_2 cm^{-2}. The calculated flux of fatty acids out of the mat during the day (16 h) and night (8 h) period amounted respectively to -0.02 and 0.15 μmol cm^{-2} for formic acid, 0.55 and 0.26 μmol cm^{-2} for acetic acid, 0.06 and 0.02 μmol cm^{-2} for propionic acid and 0.46 and 0.07 μmol cm^{-2} for lactic acid. The total daily flux of fatty acids was 3.58 μmol organic carbon cm^{-2} what corresponds to 14% of the daily gross photosynthesis and 49% of the daily net photosynthesis.

4. Discussion

Chiprana lake microbial mats are apparently rich in species. DGGE patterns of MPN dilution series revealed that specific enrichment cultures harbored a variety of numerically important species. Direct microscopic observations furthermore disclosed a high diversity of phototrophic organisms since 11 morphotypes could be distinguished. It should be realized, however, that the biodiversity estimation in our study was based for the majority on culture-based techniques. Since many organisms resist culturing in standard media, the actual biodi-

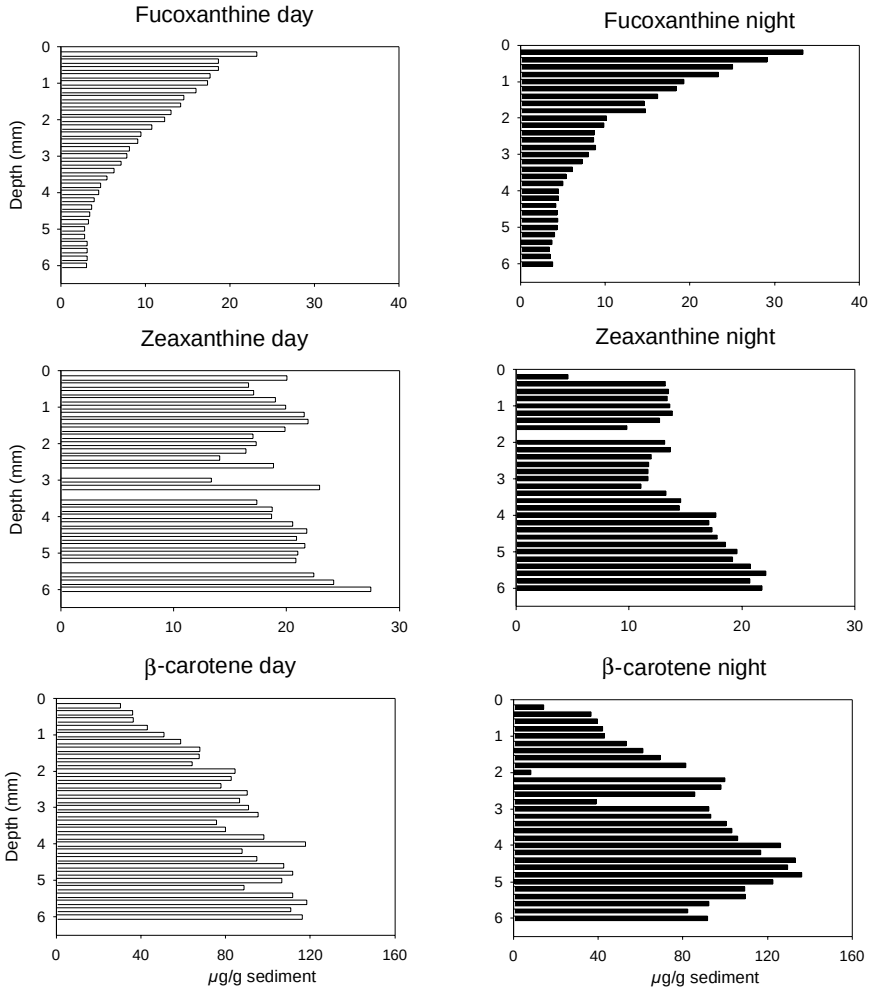

Fig. 8. Day and night depth distribution of fucoxanthin, zeaxanthine and β-carotene in Chiprana lake microbial mats, respective marker pigments for diatoms, cyanobacteria and phototrophic organisms.

versity may have been much higher. The high concentration of magnesium in Chiprana lake water, seven times higher than seawater, apparently did not restrict microbial diversity to a major extent. Whether the high magnesium concentration, that is thought to be inhibitory for many microorganisms [3], resulted in a genetically different community composition compared to other hypersaline mats remains to be investigated. We are presently constructing a clone library of 16S rDNA genes amplified from environmental DNA extracted from the Chiprana microbial mat to further investigate this matter. The structural community analysis of the Chiprana microbial mat, however, revealed conspicuous characteristics. Firstly, different morphotypes of cyanobacteria had a different depth distribution. Secondly, in Chiprana microbial mats a *Chloroflexus*-like bacteria-dominated layer was situated on top instead of below cyanobacteria-dominated layers as was reported for other *Chloroflexus*-harboring mats [25]. The *Chloroflexus*-like bacteria were the most likely source of the bacteriochlorophyll *c* homologs detected in highest concentrations in the top mm of the mat. Similar BChl*c* homologs were also observed in thalassic hypersaline microbial mats in coastal salterns [22]. *Chloroflexus aurantiacus* contains γ-carotene and β-carotene as the major carotenoid pigments [26]. The latter, but not the former, is also synthesized by cyanobacteria. The top layer of the mat contained both γ-carotene and β-carotene, a phenomenon that was also observed in the mats of the coastal solar salterns [22]. Thirdly, equal numbers of culturable sulfate-reducing bacteria were found in the photic, during the day fully oxic, top layer and underlying aphotic, permanently anoxic layer. These structural community characteristics can be explained by the functional analysis as will be discussed in the following.

The vertical distribution of photopigments in Chiprana microbial mats revealed that Chl*a* and three of its allomeres had a complementary depth distribution. Moreover, differences in day and night depth distributions, particularly of the allomeres Chla_1, Chla_2 and Chla_3, indicate that oxygenic phototrophs showed daily vertical migration behavior. Although Chl*a* allomeres are known to occur in microbial mats [15], specific depth distributions have not been reported before. Comparison with the microscopically observed depth distribution of different phototrophic

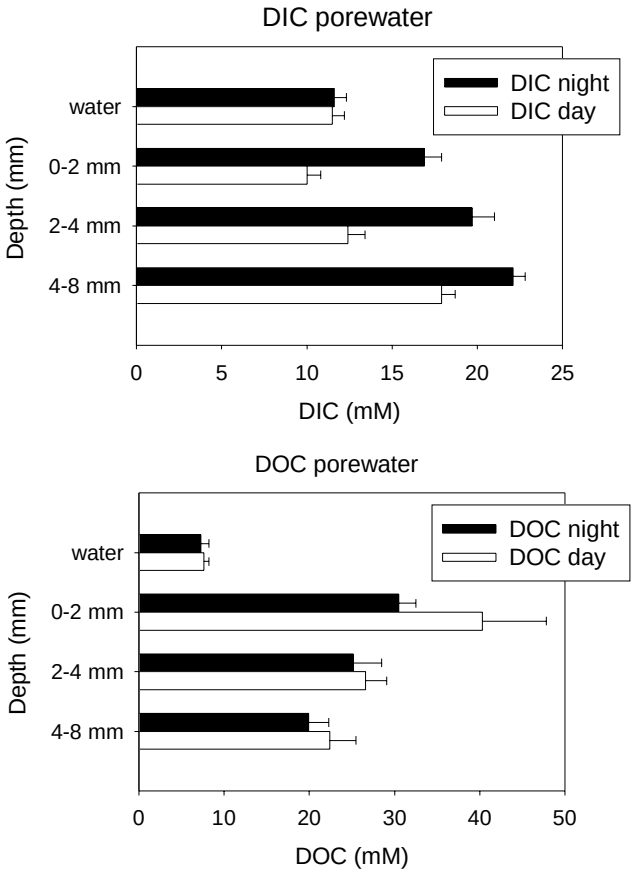

Fig. 9. Day and night porewater concentrations of dissolved organic carbon (DOC) and dissolved inorganic carbon (DIC) in Chiprana lake microbial mats. Profiles show that the 0–2 mm depth layer is reduced in DIC during the day while DOC concentrations in the mat are significantly higher than in the water column both during day and night.

morphotypes does not show a clear correlation with Chl*a* and Chl*a* allomer depth distributions. Whether the Chl*a* allomeres are species-specific photopigments or rather species-unspecific adaptations to changes in depth-related light quantity or quality remains therefore to be investigated. Alternatively, some of these Chl*a* allomers may represent diagenetic conversion products, because oxygen radicals and other compounds induce allomerization of free Chl*a* [27]. However, diagenetic conversion products are very unlikely subjected to vertical migration, unless they are carried by living organisms. Diatoms apparently did not migrate in Chiprana mats since the depth distribution of fucoxanthin, a specific carotenoid for diatoms, did not show differences between day and night. The carotenoid zeaxanthine is known to occur both in cyanobacteria and chlorophytes [27] but since the latter group also produces Chl*b* and this compound was not detected in significant amounts in Chiprana mats, it can be concluded that zeaxanthine in Chiprana mats originated from cyanobacteria. Although Chl*a* and its allomeres did show clear differences in day and night depth distributions, zeaxanthine and β-carotene did not. This can be explained by the fact that all cyanobacterial species produce zeaxanthine and most phototrophic organisms β-carotene while apparently only some of the present cyanobacterial species showed migration behavior. The amount of zeaxanthine and β-carotene translocated by the migrating cyanobacteria may thus have been obscured by the total amount of zeaxanthine and β-carotene present in the microbial mat. BChl*c* could only be detected in the top mm of the mat, an observation that is congruent with the microscopically observed depth distribution of *Chloroflexus*-like bacteria. However, concentrations were near the detection limit what hampered the determination of a more detailed depth distribution in thinner mat slices. The downward migration during the day of at least a part of the actively photosynthesizing community explains the decrease in oxygen concentration in the mat surface layer during the day at increasing light intensities. Also it explains the appearance of multiple oxygen concentration maxima in deeper parts of the microbial mat. Light-induced downward migration of cyanobacteria was also reported to occur in hypersaline mats from Guerrero Negro, Mexico, and here also only a few members of the phototrophic community actively migrated [28,29]. In these studies it was concluded that vertical migration predominantly occurred in order to escape ultraviolet light-induced damage and photo-inhibition at high levels of visible light radiation. Diatoms and *Chloroflexus*-like filamentous bacteria, which dominated the surface layer of the Chiprana lake mats, are known to be UV light resistant as they produce specific high light intensity and UV screen pigments, mycosporine-like amino acids [27] and hydroxy-γ-carotene-glucoside [25,30] respectively. These organisms do not only protect themselves but also to a certain extent the underlying microorganisms from overexposure to UV and high light intensities. In turn, as discussed below, *Chloroflexus*-like bacteria also benefit from the underlying cyanobacteria.

Both photosynthesis profiles and dissolved (in)organic carbon profiles reflect that the highest primary production rates occurred in the 0–2 mm surface layer of the mat. Here, inorganic carbon concentration was low during the day while in the overlaying water and in deeper sediment layers concentrations were higher. This means that during the day a flux of dissolved inorganic carbon occurred both from above and from below towards this layer. At night however, inorganic carbon concentration increased with increasing sediment depth meaning that a flux of inorganic carbon from the mat to the overlaying water occurred, a phenomenon that was expected because at night mineralization generally exceeds carbon dioxide fixation. Interestingly, dissolved organic carbon profiles show that Chiprana mats produced organic carbon both during the day and at night because concentrations in porewater were always higher than in the overlaying water. Although some organic carbon that is produced in the 0–2 mm depth layer diffuses towards deeper layers in the mat, the main flow of dissolved organic carbon will be towards the overlaying

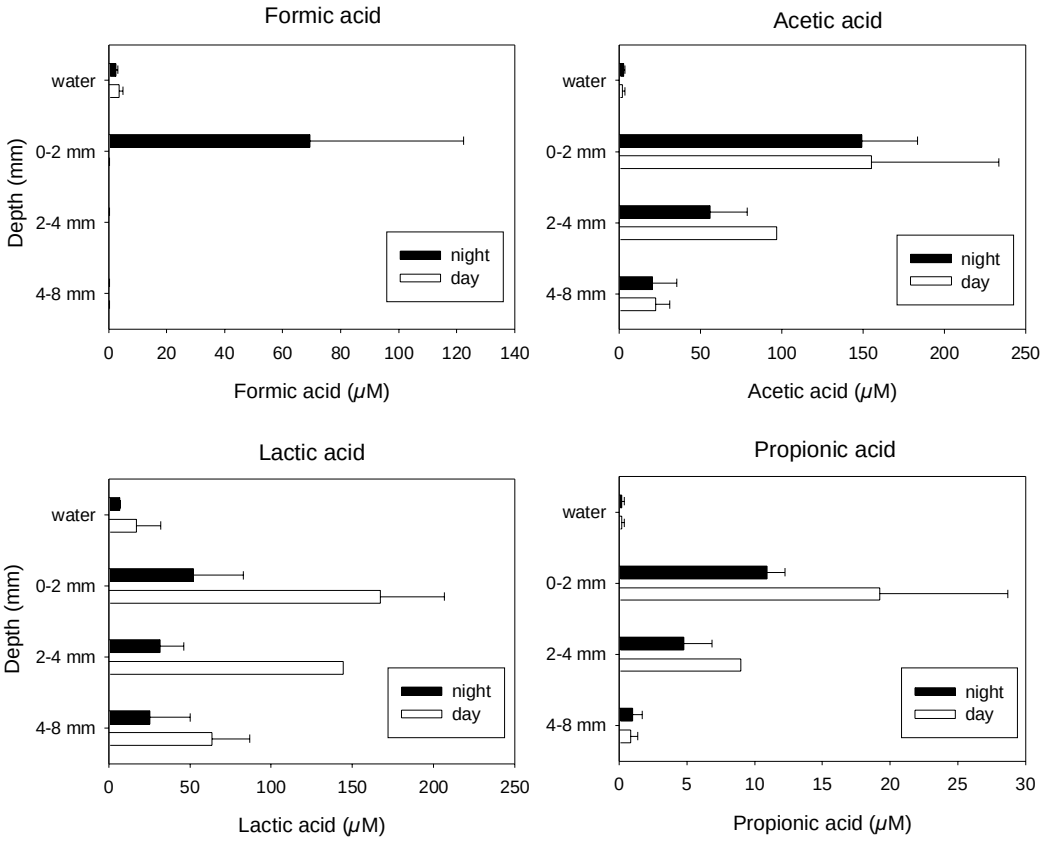

Fig. 10. Day and night porewater concentrations of formic, acetic, lactic, and propionic acid. Except for formic acid, day time concentrations are higher than night time concentrations in all mat layers.

water since the difference in concentration is much higher between these two. In this study it was estimated that although low molecular mass fatty acids make up only 2% of the porewater DOC pool, the daily flux of these compounds from the mat to the water column amounts to 14% of the daily gross photosynthesis and 49% of the daily net photosynthesis. The as yet unidentified fraction of the DOC pool probably consists for the major part of polymeric compounds such as polysaccharides and proteins. These larger molecules have typically much smaller diffusion coefficients and are therefore less mobile. Although the contribution of the latter compounds to the DOC pool may be much higher, the flux out of the mat may be much smaller than that of low molecular mass fatty acids. The main flow direction of the DOC compounds explains why in Chiprana mats the *Chloroflexus*-like bacteria grow on top instead of below the cyanobacterial layers. Here they can maximally benefit from the flow of organic photosynthases excreted by oxygenic primary producers which are the preferred substrates of these photoheterotrophic organisms [31]. The DOC profiles furthermore strongly suggest that primary production in Chiprana mats is nutrient limited. Oxygenic primary producers are known to direct the flow of reduced photosynthetic carbon towards the production of extracellular polymeric substances and low molecular mass organic compounds instead to structural cell components under nutrient-limiting conditions [32,33]. Significant concentrations of acetic, lactic and propionic acid, typical substrates for sulfate-reducing bacteria, were detected both in day and night porewater samples. This may explain why sulfate-reducing bacteria occur in relatively high numbers in the oxic surface layer because they apparently do not have to compete with aerobic heterotrophic bacteria for substrates. Moreover, as recent findings indicate, sulfate-reducing bacteria can tolerate high oxygen concentrations but need occasional periods of anoxia for good growth [34], conditions that occur in the major part of the photic zone during the night. Although future analyses have to clarify what the nature and identity of the compounds are that make up the major fraction of the dissolved organic carbon pool, it can be concluded that a large fraction of the oxygenic primary production in Chiprana microbial mats leaves the system as dissolved organic carbon and is not used for biomass synthesis.

This study showed that the benthic microbial mats of Chiprana lake not only represent an excellent model ecosystem for the study of biogeochemical processes but it is also an original and diverse benthic microbial ecosystem, the study of which may contribute to a better understanding of ecological, physiological and genetic questions. Efforts should therefore be undertaken to protect the unique Chiprana lake ecosystem in order to conserve its still largely unexplored biodiversity.

Acknowledgements

We are indebted to the local authorities in Chiprana for granting permission to access the lake and take microbial mat samples and we are particularly grateful to Alfredo Legaz (Guard) for support during field work. Axel Schippers and Kirsten Neumann are thanked for their help with sample analysis and Gerhard Holst for photographing microbial mat samples.

References

[1] Bauld, J. (1981) Occurrence of benthic microbial mats in saline lakes. Hydrobiology 81, 87–111.
[2] Williams, W.D. (1986) Limnology, the study of inland waters: a comment on perceptions of studies on salt lakes, past and present. In: Limnology in Australia (De Deckker, P. and Williams, W.D., Eds.), pp. 471–496. Dr. W. Junk Publisher, Dordrecht.
[3] Guerrero, M.C. and De Wit, R. (1992) Microbial mats in the inland saline lakes of Spain. Limnetica 8, 197–204.
[4] Valero-Garces, B.L., Navas, A., Machin, J., Stevenson, T. and Davis, B. (2000) Responses of a saline lake ecosystem in a semiarid region to irrigation and climate variability – The history of Salada Chiprana, central Ebro basin, Spain. Ambio 29, 344–350.
[5] Vidondo, B., Martinez, B., Montes, C. and Guerrero, M.C. (1993) Physicochemical characteristics of a permanent Spanish hypersaline lake – La-Salada-De-Chiprana (Ne Spain). Hydrobiology 267, 113–125.
[6] Diaz, P., Guerrero, M.C., Alcorlo, P., Baltanas, A., Florin, M. and Montes, C. (1998) Anthropogenic perturbations to the trophic structure in a permanent hypersaline shallow lake: La Salada de Chiprana (north-eastern Spain). Int. J. Salt Lake Res. 7, 187–210.
[7] Vila, X., Guyoneaud, R., Cristina, X.P., Figueras, J.B. and Abella, C.A. (2002) Green sulfur bacteria from hypersaline Chiprana Lake (Monegros, Spain): habitat description and phylogenetic relationships of isolated strains. Photosynth. Res. 71, 165–172.
[8] Clarke, T. and Owens, N. (1983) A simple and versatile micro-computer program for the determination of 'most probable number'. J. Microbiol. Methods 1, 133–137.
[9] Widdel, F. and Bak, F. (1992) Gram-negative mesophilic sulfate-reducing bacteria. In: The Prokaryotes, 2nd Edn. (Balows, A., Truper, H.G., Dworkin, M., Harder, W. and Schleifer, K.H., Eds.), pp. 3353–3378. Springer, New York.
[10] Heijthuijsen, J. and Hansen, T.A. (1986) Interspecies hydrogen transfer in cocultures of methanol-utilizing acidogens and sulfate-reducing or methanogenic bacteria. FEMS Microbiol. Ecol. 38, 57–64.
[11] Muyzer, G., Teske, A., Wirsen, C.O. and Jannasch, H.W. (1995) Phylogenetic-relationships of *Thiomicrospira* species and their identification in deep-sea hydrothermal vent samples by denaturing gradient gel-electrophoresis of 16s rDNA fragments. Arch. Microbiol. 164, 165–172.
[12] Revsbech, N.P. (1994) Analysis of microbial mats by use of electrochemical microsensors: recent advances. In: Microbial Mats (Stal, L.J. and Caumette, P., Eds.), pp. 135–147. NATO ASI Series Vol. G35, Springer, Berlin.
[13] Kuhl, M., Steuckart, C., Eickert, G. and Jeroschewski, P. (1998) A H_2S microsensor for profiling biofilms and sediments: application in an acidic lake sediment. Aquat. Microb. Ecol. 15, 201–209.
[14] Revsbech, N.P. and Jørgensen, B.B. (1983) Photosynthesis of benthic microflora measured with high spatial resolution by the oxygen microprofile method: capabilities and limitations of the method. Limnol. Oceanogr. 28, 749–756.
[15] Buffan-Dubau, E., Pringault, O. and De Wit, R. (2001) Artificial cold-adapted microbial mats cultured from Antarctic lake samples. 1. Formation and structure. Aquat. Microb. Ecol. 26, 115–125.
[16] Wright, S.W., Jeffrey, S.W., Mantoura, R.F.C., Llewellyn, C.A., Bjornland, T., Repeta, D. and Welschmeyer, N. (1991) Improved HPLC method for the analysis of chlorophylls and carotenoids from marine phytoplankton. Mar. Ecol. Prog. Ser. 77, 183–196.
[17] Albert, D.B. and Martens, C.S. (1997) Determination of low-molecular-weight organic acid concentrations in seawater and porewater samples via HPLC. Mar. Chem. 56, 27–37.
[18] Schippers, A. and Jørgensen, B.B. (2001) Oxidation of pyrite and iron sulfide by manganese dioxide in marine sediments. Geochim. Cosmochim. Acta 65, 915–922.
[19] Jeffrey, S., Mantoura, R. and Björnland, T. (1997) Phytoplankton Pigments in Oceanography: Guidelines to Modern Methods. UNESCO Publishing, Paris.
[20] Borrego, C.M. and Garcia-Gil, L.J. (1994) Separation of bacteriochlorophyll homologues from green photosynthetic bacteria by reversed-phase HPLC. Photosynth. Res. 41, 157–163.
[21] Airs, R.L., Atkinson, J.E. and Keely, B.J. (2001) Development and application of a high resolution chromatographic method for the analysis of complex pigment distributions. J. Chromatogr. A 917, 167–177.
[22] Villanueva, J., Grimalt, J.O., De Wit, R., Keely, B.J. and Maxwell, J.R. (1994) Chlorophyll and carotenoid pigments in solar saltern microbial mats. Geochim. Cosmochim. Acta 56, 4703–4715.
[23] Revsbech, N.P., Jørgensen, B.B., Blackburn, T.H. and Cohen, Y. (1983) Microelectrode studies of the photosynthesis and O_2, H_2S, and pH profiles of a microbial mat. Limnol. Oceanogr. 28, 1062–1074.
[24] Perry, R. and Green, D. (1984) Diffusion coefficients. In: Perry's Chemical Engineers' Handbook, 6th Edn. (Crawford, H. and Eckes, B., Eds.), pp. 3/285–283/287. McGraw-Hill, Singapore.
[25] Pierson, B. and Castenholz, R. (1992) The family *Chloroflexaceae*. In: The Prokaryotes, 2nd Edn. (Balows, A., Trüper, H., Dworkin, M., Harder, W. and Schleifer, K., Eds.). Springer, New York.
[26] Schmidt, K. (1978) Biosynthesis of carotenoids. In: The Photosynthetic Bacteria (Calyton, R.K. and Sistrom, W.R., Eds.), pp. 729–750. Plenum Press, New York.
[27] Jeffrey, S.W., MacTavish, H.S., Dunlap, W.C., Vesk, M. and Groenewoud, K. (1999) Occurrence of UVA- and UVB-absorbing compounds in 152 species (206 strains) of marine microalgae. Mar. Ecol. Prog. Ser. 189, 35–51.
[28] Garcia-Pichel, F., Mechling, M. and Castenholz, R.W. (1994) Diel migrations of microorganisms within a benthic, hypersaline mat community. Appl. Environ. Microbiol. 60, 1500–1511.
[29] Kruschel, C. and Castenholz, R.W. (1998) The effect of solar UV and visible irradiance on the vertical movements of cyanobacteria in microbial mats of hypersaline waters. FEMS Microbiol. Ecol. 27, 53–72.
[30] Pierson, B.K., Mitchell, H.K. and Ruffroberts, A.L. (1993) *Chloroflexus aurantiacus* and ultraviolet-radiation – implications for archean shallow-water stromatolites. Orig. Life Evol. Biosph. 23, 243–260.
[31] Bateson, M.M. and Ward, D.M. (1988) Photoexcretion and fate of glycolate in a hot-spring cyanobacterial mat. Appl. Environ. Microbiol. 54, 1738–1743.
[32] Hoagland, K.D., Rosowski, J.R., Gretz, M.R. and Roemer, S.C. (1993) Diatom extracellular polymeric substances – function, fine-structure, chemistry, and physiology. J. Phycol. 29, 537–566.
[33] Stal, L.J. (1995) Physiological ecology of cyanobacteria in microbial mats and other communities. N. Phytol. 131, 1–32.
[34] Cypionka, H. (2000) Oxygen respiration by *Desulfovibrio* species. Annu. Rev. Microbiol. 54, 827–848.
[35] Stumm, W. and Morgan, J. (1996) Aquatic Chemistry, 3rd Edn. Wiley, New York.